

# Propagation and Termination Processes in the Free-Radical Copolymerization of Methyl Methacrylate and Vinyl Acetate

Yung-Dae Ma\* and You-Chan Won†

Department of Polymer Science and Engineering, Dankook University, San 8, Hannam-dong, Yongsan-ku, Seoul 140, Korea

Keiji Kubo‡ and Takeshi Fukuda\*

Institute for Chemical Research, Kyoto University, Uji, Kyoto 611, Japan

Received July 28, 1993\*

**ABSTRACT:** The propagation and termination processes in free-radical copolymerization were examined on the basis of a complete set of experimental data carefully obtained for the bulk copolymerization of methyl methacrylate (MMA) and vinyl acetate (VAc) at 40 °C by use of the rotating-sector technique. The composition curve conformed to the terminal model within experimental error. However, a moderate penultimate-unit effect was observed for the terminal MMA radical ( $s_1 = k_{211}/k_{111} = 0.4 \pm 0.2$ ), in conformity to the prediction of the stabilization energy model. The concentration of the terminal VAc radical was too small to elucidate the details about this radical. The termination process in this system conforms to the notion of diffusion control, but the North diffusion model was found inadequate. Alternative, simple, no-parameter models were proposed, which described the experiments better.

## Introduction

Recent experimental studies have disclosed a fundamental defect of the classical notion of free-radical copolymerization.<sup>1-10</sup> Namely, it was observed in many systems that the terminal model or the Mayo-Lewis scheme<sup>11</sup> fails to predict absolute values of the propagation rate constant  $\bar{k}_p$  of copolymerization, while it describes the composition (and sequence distribution) formally well. This phenomenon was shown<sup>3</sup> to originate in a penultimate-unit effect (PUE) and led to the postulate that radical stabilization energies are influenced by penultimate units.<sup>12,13</sup> This "stabilization energy model" predicts the simple relation

$$r_1 r_2 = s_1 s_2 \quad (1)$$

where  $r_1$  and  $r_2$  are the monomer reactivity ratios, which, according to this model, are independent of composition, and  $s_1$  and  $s_2$  are the radical reactivity ratios defined by  $s_1 = k_{211}/k_{111}$  and  $s_2 = k_{122}/k_{222}$ , with  $k_{ijm}$  being the rate constant of the reaction of radical  $\sim \sim \sim ij^*$  with monomer  $m$  ( $i, j, m = 1$  or  $2$ ). This correlation of  $r_i$  and  $s_i$  seems to exist actually.<sup>14,15</sup>

In this paper, we present a complete set of experimental data carefully collected for the bulk copolymerization of methyl methacrylate (MMA) and vinyl acetate (VAc) at 40 °C by use of the rotating-sector technique.<sup>1</sup> Most of the systems previously studied with respect to  $\bar{k}_p$  involved styrene or its derivative as a comonomer. It will be important to study non-styryl systems, too, to obtain a more general understanding. According to eq 1, the MMA/VAc system ( $r_1 r_2 = 0.39$ , see below) should show a moderate PUE.

Another interest in this system concerns the termination process. Previous studies have shown that the termination step in copolymerization is, like in homopolymerization, diffusion controlled,<sup>1-4,16</sup> but details are still unknown. The termination rate constant of VAc<sup>17-19</sup> is more than an

order of magnitude larger than that of MMA. This makes model discrimination much easier than in other systems. It will be rather conclusively shown here that the North diffusion model is inadequate to describe this system. A preliminary brief account of this work has been presented in a review article.<sup>15</sup>

## Experimental Section

Commercially obtained monomers MMA and VAc (Wako Chemical Co., Japan), initiators 2,2'-azobis(isobutyronitrile) (AIBN) and 2,2'-azobis(cyclohexane-1-carbonitrile) (ACN; Nacalai Chemicals, Japan), and inhibitor 4-hydroxy-2,2,6,6-tetramethylpiperidiny-1-oxy (HTMPO; Eastman Kodak Co., Rochester, NY) were purified as described previously.<sup>1</sup>

The compositions of MMA-VAc copolymers were determined by <sup>1</sup>H nuclear magnetic resonance (NMR) on a JEOL PM × 60SI spectrometer. Representative spectra are shown in Figure 1.

Other experiments performed involved determining the initiation rate, the volume contraction factor, the steady-state polymerization rate, and the radical lifetime, as a function of feed monomer composition  $f_1$ . Each experiment was carried out as described previously.<sup>1,4</sup> Care was taken to keep conversions low enough so that composition drifts with conversion may be neglected. This was important particularly for low- $f_1$  runs ( $f_1 < 0.05$ ), for which drastic changes in the copolymerization rate and copolymer composition  $F_1$  were expected to accompany a small change in  $f_1$ .

## Results

**Volume Contraction Factor.** The volume contraction factor  $\Gamma^\circ$ , defined as the decrease of the system volume (in milliliters) per unit mole of the monomer mixture converted to polymer at zero polymer concentration, was calculated according to the equation previously proposed.<sup>1</sup> Values of the relevant parameters were determined by density measurements and are reported in Table I. The values of  $\Gamma^\circ$  thus estimated should be correct to  $\pm 1\%$ .

**Initiation Rate.** The initiation rate  $R_i$  for the AIBN initiator was determined by the inhibition method using HTMPO. Well-defined inhibition times were obtained in all cases with  $f_1 = 0-1$ . As Table II shows, the effective initiator decomposition rate constant  $2f''k_d$  in this system

\* To whom correspondence should be addressed.

† Present address: Daeduck Industrial Co., Ltd., 475, Mognae-dong, Ansanshi, Kyunggi-do 425-100, Korea.

‡ Present address: Kuraray Co., Ltd., Kurashiki, Okayama 715, Japan.

\* Abstract published in *Advance ACS Abstracts*, October 15, 1993.

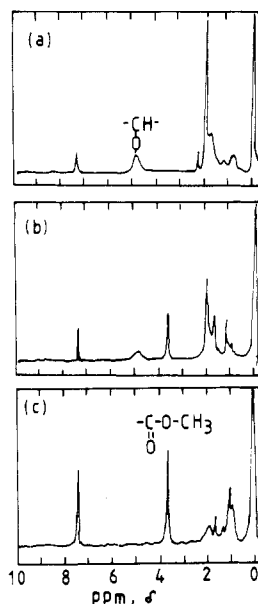


Figure 1.  $^1\text{H}$ -NMR spectra of (a) VAc, (b) MMA-VAc copolymer ( $f_1 = 0.11$ ), and (c) MMA, in  $\text{CDCl}_3$ .

Table I. Values of the Volumetric Parameters for the MMA(1)/VAc(2)/40 °C System<sup>a</sup>

$V_1$	108.61	$\bar{V}_{1,1}$	81.20
$V_2$	95.00	$\bar{V}_{1,2}$	81.70
$10^3 a_{12}$	-2.60	$\bar{V}_{2,2}$	71.98
$\Delta V_{12}$	2.90	$\bar{V}_{2,1}$	71.55

<sup>a</sup> For the symbols, see ref 1:  $V$ 's and  $\Delta V_{12}$  are in  $\text{mL mol}^{-1}$ .

Table II. Inhibition Times of the MMA/VAc/AIBN/HTMPO/40 °C System

$f_1^a$	$10^2[\text{AIBN}]$ ( $\text{mol L}^{-1}$ )	$10^4[\text{HTMPO}]$ ( $\text{mol L}^{-1}$ )	$t_i^b$ (min)	$10^6(2f'k_d)$ ( $\text{s}^{-1}$ )
0.000	4.902	2.170	135	0.547
0.111	4.782	2.045	136	0.525
0.193	6.592	3.751	175	0.542
0.294	5.870	2.704	143	0.537
0.405	7.005	3.969	181	0.522
0.426	4.620	2.086	143	0.526
0.572	5.398	3.650	217	0.519
0.636	4.778	2.207	140	0.549
0.772	6.930	3.787	170	0.536
0.871	4.777	2.123	141	0.525
1.000				0.535 <sup>c</sup>

<sup>a</sup> Mole fraction of MMA. <sup>b</sup> Inhibition time. <sup>c</sup> From ref 1.

depends very little on  $f_1$  and can be given by

$$2f'k_d \times 10^6 = 0.547 - 0.012f_1 \quad (\text{in s}^{-1}) \quad (2)$$

**Steady-State Polymerization.** The overall copolymerization rate  $R_p$  is given by

$$R_p = (\bar{k}_p/\bar{k}_t^{1/2})R_i^{1/2}[M] \quad (3)$$

$$R_i = 2f'k_d[I] \quad (4)$$

where  $\bar{k}_p$  and  $\bar{k}_t$  are the rate constants of propagation and termination, respectively, and  $[M]$  and  $[I]$  are the concentrations of the monomer mixture and initiator, respectively. Figure 2 confirms the proportionality of  $R_p$  to  $[I]^{1/2}$  for two values of  $f_1$ . Results of steady-state copolymerization are summarized in Table III.

Figure 3 demonstrates the plot of  $\bar{k}_p/\bar{k}_t^{1/2}$  vs  $f_1$ . It can be seen that  $\bar{k}_p/\bar{k}_t^{1/2}$  decreases drastically with decreasing  $f_1$ , showing an increasing tendency only at very small  $f_1$ . The solid curve in the figure is a best-fit representation of the data and will be used for the following analysis.

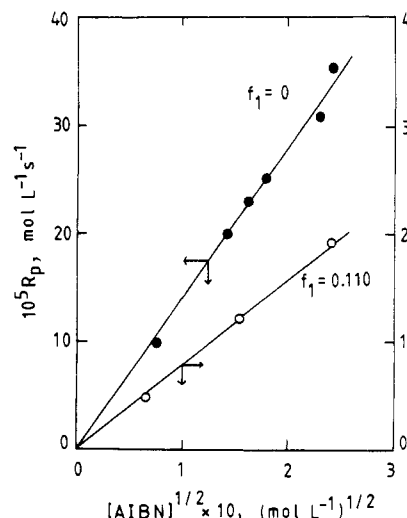


Figure 2. Plot of  $R_p$  vs  $[\text{AIBN}]^{1/2}$  for the MMA/VAc/AIBN/40 °C system.

Table III. Summary of the Steady-State Copolymerization of MMA and VAc in the Bulk at 40 °C

run	$f_1^a$	$[\text{M}]^b$ ( $\text{mol L}^{-1}$ )	$10^2[\text{I}]^c$ ( $\text{mol L}^{-1}$ )	$Y^d$ (wt %)	$t^e$ (min)	$F_1^f$	$10^4 R_p/[\text{I}]^{1/2}$ ( $\text{mol L}^{-1/2} \text{s}^{-1}$ )
1	0.000	10.526	2.036				14.020 <sup>g,h</sup>
2			0.586				
3			2.644				
4			3.164				
5			5.273				
6			5.787				
7	0.023	10.492	2.026	0.56	118	0.512	0.540
8	0.055	10.444	2.224	0.85	240	0.669	0.380
9	0.062	10.434	2.556	1.02	240	0.713	0.424
10	0.085	10.400	1.898	1.99		0.760	
11	0.110	10.364	0.423				0.782 <sup>g,h</sup>
12			2.416				
13			5.836				
14	0.138	10.332	2.807	1.19	129		0.857
15	0.201	10.231	3.280	3.52		0.872	
16	0.274	10.129	2.697	1.80	117	0.929	1.441
17	0.357	10.013	3.121	2.11	109	0.951	1.682
18	0.426	9.921	4.620				2.157 <sup>i</sup>
19	0.525	9.791	3.012	4.79	182	0.958	2.660
20	0.539	9.771	2.936	3.14	111	0.974	2.529
21	0.572	9.728	5.398				2.843 <sup>j</sup>
22	0.649	9.631	3.016	3.74	110	0.982	3.145
23	0.735	9.524	2.562	3.82	103	0.987	3.550
24	0.871	9.380	4.777				3.998
25	1.000						4.626 <sup>i</sup>

<sup>a</sup> Mole fraction of MMA in the feed. <sup>b</sup> Total monomer concentration. <sup>c</sup> AIBN concentration. <sup>d</sup> Conversion. <sup>e</sup> Reaction time. <sup>f</sup> Mole fraction of MMA in the copolymer. <sup>g</sup> By dilatometry. <sup>h</sup> Average value. <sup>i</sup> Reference 1.

**Radical Lifetime.** Rotating-sector experiments were carried out at a dark-to-light time ratio of 2. Some raw experimental data are presented in Figure 4. A well-defined lifetime  $\tau$  could be determined for all values of  $f_1$  examined. The results are summarized in Table IV.

## Discussion

**Composition Curve.** Reported  $r_1$  and  $r_2$  values of the MMA/VAc system are considerably scattered,<sup>21</sup> and some of those  $r_2$  values are even negative, implying the inapplicability of the terminal-model scheme.

Figure 5a shows the composition curve obtained in this work. The data were fitted to the Mayo-Lewis equation<sup>11</sup> by a least-squares method to obtain the solid curve in the figure with  $r_1 = 27.8$  and  $r_2 = 0.014$ . The differences between the observed and calculated compositions are magnified in Figure 5b, in which no deviations exceeding

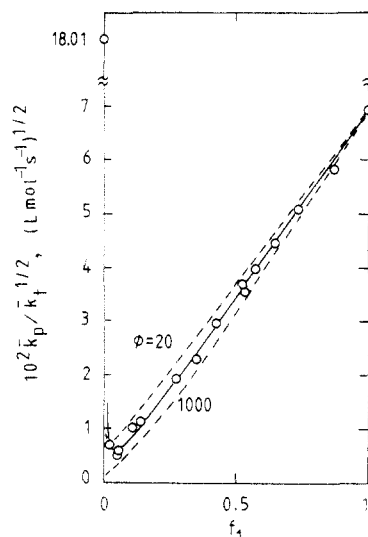


**Figure 3.** Plot of  $\bar{k}_p/\bar{k}_t^{1/2}$  vs  $f_1$  for the MMA/VAc/AIBN/40 °C system. The solid curve is the best-fit representation of the experimental data shown by the circles. The broken curves represent the Walling equation<sup>1</sup> with the values of  $\phi$  indicated in the figure.

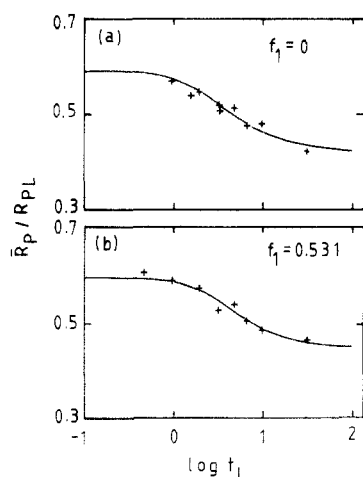


**Figure 4.** Plot of  $\bar{R}_p/\bar{R}_{pL}$  vs  $\log t_L$  for the MMA/VAc/ACN/40 °C system: (a)  $f_1 = 0$ ,  $[\text{ACN}] = 0.356 \times 10^{-3} \text{ mol L}^{-1}$ , and  $R_{pD}/R_{pL} = 0.128$  ( $\tau = 1.40 \text{ s}$ , the solid curve); (b)  $f_1 = 0.531$ ,  $[\text{ACN}] = 9.25 \times 10^{-3} \text{ mol L}^{-1}$ , and  $R_{pD}/R_{pL} = 0.172$  ( $\tau = 1.77 \text{ s}$ ), where  $t_L$  is the duration of the light period, and  $R_{pL}$ ,  $R_{pD}$ , and  $\bar{R}_p$  are the polymerization rates in the light, in the dark, and with intermittent illumination, respectively.

**Table IV.** Summary of the Rotating-Sector Experiments for the MMA(1)/VAc(2)/40 °C System

$f_1$	$10^3[\text{ACN}]$ (mol L <sup>-1</sup> )	$10^5 R_{pL}$ (mol L <sup>-1</sup> s <sup>-1</sup> )	$R_{pD}/R_{pL}$	$\tau$ (s)
0.000	0.305	4.350	0.137	1.16
	0.356	4.058	0.128	1.40
	0.420	4.082	0.123	1.38
0.042	20.866	0.847	0.169	0.97
0.060	24.307	0.947	0.151	1.46
0.110	16.610	1.418	0.172	1.12
0.207	20.374	1.776	0.138	1.86
0.286	20.728	2.287	0.130	1.55
0.350	10.590	2.898	0.159	1.81
0.531	9.250	4.263	0.172	1.77
0.704	7.390	4.130	0.196	2.12

experimental uncertainty (about  $\pm 1.5\%$ ) or a systematic trend can be observed. Thus the composition curve of this system may be described by the terminal model, at least to a good approximation.

**Propagation Process.** The values of  $\bar{k}_p$  obtained by combining the  $\bar{k}_p/\bar{k}_t^{1/2}$  and  $\bar{k}_p/\bar{k}_t$  data are listed in Table

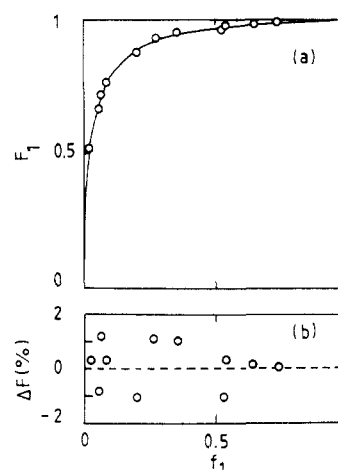


**Figure 5.** (a) Plot of  $F_1$  vs  $f_1$  for MMA/VAc copolymers. The solid curve represents the Mayo-Lewis equation with  $r_1 = 27.8$  and  $r_2 = 0.014$ . (b) Plot of  $\Delta F = F_{1,\text{obsd}} - F_{1,\text{calcd}}$  vs  $f_1$ .

**Table V.** Values of  $\bar{k}_p$  and  $\bar{k}_t$  for the MMA(1)/VA(2)/40 °C System

$f_1$	$10^2(\bar{k}_p/\bar{k}_t^{1/2})^b$ [(L mol <sup>-1</sup> s <sup>-1</sup> ) <sup>1/2</sup> ]	$10^5(\bar{k}_p/\bar{k}_t)$ (L mol <sup>-1</sup> s <sup>-1</sup> )	$\bar{k}_p$ (L mol <sup>-1</sup> s <sup>-1</sup> )	$10^{-7}\bar{k}_t$ (L mol <sup>-1</sup> s <sup>-1</sup> )
0.000	18.01	0.479	6800	140
		0.540	6000	110
		0.535	6100	110
0.042	0.58	0.079	43	5.4
0.060	0.62	0.132	29	2.2
0.110	0.87	0.153	49	3.2
0.207	1.45	0.323	65	2.0
0.286	1.97	0.352	110	3.1
0.350	2.40	0.523	110	2.1
0.531	3.64	0.771	172	2.2
0.704	4.84	0.915	256	2.8
1.000 <sup>c</sup>	6.92	1.26	377	3.0

<sup>a</sup> The viscosity  $\eta$  of this system is given by  $\eta = 0.455f_1 + 0.340f_2$  (in cP). <sup>b</sup> Value read from the solid curve in Figure 3. <sup>c</sup> From ref 1.

V. One of the notable features of this system is the extremely large  $k_p$  exhibited by one of the pure monomers, VAc ( $k_p = 6300 \text{ L mol}^{-1} \text{ s}^{-1}$  at 40 °C). This value is considerably larger than those obtained by Atherton and North (988 at 30 °C and 3600 at 60 °C)<sup>20</sup> but nearly consistent with the value due to Yamamoto et al. (3500 at 30 °C),<sup>18</sup> if the temperature difference is taken into account. In the examined range of composition ( $f_1 \geq 0.042$ ), the  $\bar{k}_p$  values are smaller than the VAc value by 1 or 2 orders of magnitude.

In Figure 6,  $\bar{k}_p$  is plotted as a function of  $f_1$  and compared to the prediction by the terminal model:<sup>1</sup>

$$\bar{k}_p = \frac{r_1 r_1^2 + 2f_1 f_2 + r_2 f_2^2}{r_1 f_1 / k_{11} + r_2 f_2 / k_{22}} \quad (5)$$

Evidently, the experimental points show deviations from the model. These deviations are not very large but quite systematic, and some of them exceed the experimental error limit of  $\pm 20\%$ .<sup>1</sup> Thus we conclude that the propagation step of this system does not obey the terminal model.

The  $k_p$  of VAc has been known to show a strong solvent effect.<sup>17-19</sup> For example, it was observed that the  $k_p$  in the solutions with aromatic solvents like benzene and chlorobenzene becomes smaller by an order of magnitude (or more) than in the bulk,<sup>18</sup> or in ethyl acetate,<sup>17</sup> and this phenomenon has been interpreted in terms of a reversible complex formation between the propagating radical and aromatic solvents.<sup>17,19</sup> In the bulk copolymerization of VAc and MMA, which involves no aromatic molecules,

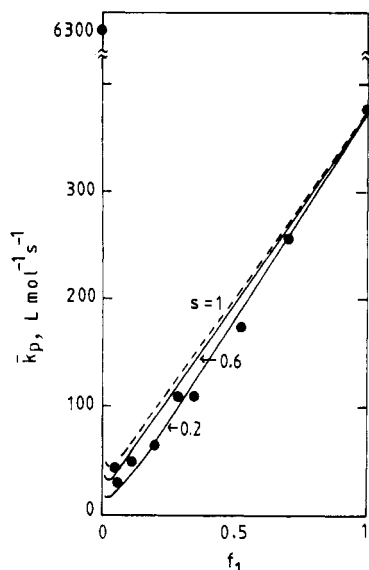


**Figure 6.** Plot of  $\bar{k}_p$  vs  $f_1$  for the MMA/VAc/40 °C system: the circles were measured, and the solid curves represent the penultimate model with  $r_1 = 27.8$ ,  $r_2 = 0.014$ ,  $k_{11} = 377 \text{ mol L}^{-1} \text{ s}^{-1}$ ,  $k_{22} = 6300 \text{ mol L}^{-1} \text{ s}^{-1}$ , and  $s (=s_1 = s_2)$  as indicated in the figure. The broken curve shows the terminal model ( $s = 1$ ).

such a drastic environmental effect is not expectable. Moreover, since  $r_2$  is about 1/2000 of  $r_1$  (see above), it is clear from eq 5 that the  $\bar{k}_p$  is totally independent of the value of  $k_{22}$  in the studied range of  $f_1$  ( $\geq 0.04$ ), only if  $k_{22} \geq k_{11}$ . In other words, even if the  $k_{22}$  in a given monomer mixture should be reduced by a factor of 1/20 from the bulk value for some reason or another, the value of  $\bar{k}_p$  would remain virtually constant. A "solvent effect" on  $k_{11}$  is more hardly expectable for this system. For these reasons, the observed failure of the terminal model should be ascribed to a PUE, not to an environment effect.<sup>3</sup>

The penultimate-model expression for  $\bar{k}_p$  is given by eq 5 with  $k_{11}$  and  $k_{22}$  replaced by  $\bar{k}_{11}$  and  $\bar{k}_{22}$ .<sup>1,4</sup>

$$\bar{k}_{11} = k_{111}(r_1 f_1 + f_2)/(r_1 f_1 + s_1^{-1} f_2) \quad (6)$$

$$\bar{k}_{22} = k_{222}(r_2 f_2 + f_1)/(r_2 f_2 + s_2^{-1} f_1) \quad (7)$$

where  $r_1$  and  $r_2$  are assumed to be constant (see above), and  $k_{111}$  and  $k_{222}$  denote the rate constants of the homopolymerizations. As mentioned above, the  $\bar{k}_p$  of this system is insensitive to  $k_{22}$ , which, in turn, means that it is absolutely impossible to determine the value of  $s_2$ . For this reason, we simply assume that  $s_1 = s_2 = s$ . The two solid curves in Figure 6 represent the penultimate model with  $s = 0.6$  and  $0.2$ , respectively. Most of the experimental points lie between them, and we estimate that  $s_1 = 0.4 \pm 0.2$ , leaving  $s_2$  undetermined. This magnitude of PUE appears to be in line with the prediction of the stabilization energy model (see the Introduction).

**Termination Process.** Previous studies have clearly shown that the termination step of radical copolymerization should be understood as a diffusion-controlled process.<sup>1-4</sup> Hence, this process is relevant to the molecular or segmental motions of growing radicals, and this poses a physical problem that is particularly difficult to solve in a rigorous sense. Several approximate treatments have been proposed, of which the model of Atherton and North<sup>20</sup> assumes that  $\bar{k}_t$  depends on the mean composition of the copolymer such that

$$\bar{k}_t = F_1 k_{t1} + F_2 k_{t2} \quad (\text{model 1}) \quad (8)$$

where the  $k_{ti}$ s refer to the homopolymerizations. As another extreme case, one could assume that  $\bar{k}_t$  depends

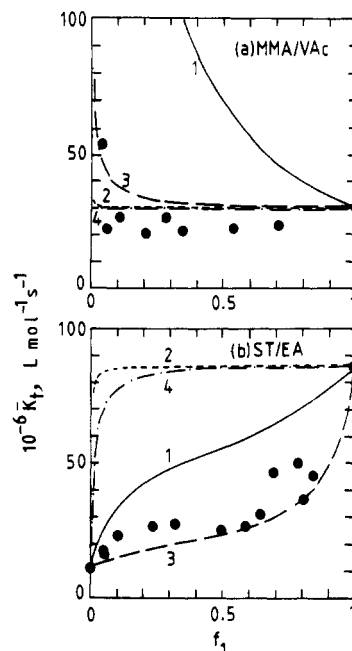


**Figure 7.** Plot of  $\bar{k}_t$  vs  $f_1$  for (a) MMA/VAc/40 °C and (b) ST/EA/40 °C systems. The circles were measured, and curves 1–4 represent the termination models 1–4, respectively (see text).

only on the "composition" of the active terminal unit. By analogy to eq 8, one could write

$$\bar{k}_t = P_1 k_{t1} + P_2 k_{t2} \quad (\text{model 2}) \quad (9)$$

where  $P_i$  ( $P_1 + P_2 = 1$ ), the relative population of radical  $i$ , can be known, provided the propagation model is known: for the penultimate model with composition-independent  $r_1$  and  $r_2$ ,  $P_i$  is given by

$$P_1/P_2 = r_1 f_1 / \bar{k}_{11} / r_2 f_2 / \bar{k}_{22} \quad (10)$$

In a previous paper,<sup>4</sup> we have proposed another simple model that appears to be physically more realistic than model 1:

$$\bar{k}_t^{-1} = F_1 k_{t1}^{-1} + F_2 k_{t2}^{-1} \quad (\text{model 3}) \quad (11)$$

This model is based on the averaging of the friction coefficient of the copolymer molecule with respect to the composition. Similarly, the averaging of the friction coefficient of the terminal unit gives model 4, as an alternative to model 2:

$$\bar{k}_t^{-1} = P_1 k_{t1}^{-1} + P_2 k_{t2}^{-1} \quad (\text{model 4}) \quad (12)$$

No adjustable parameter is involved in any of these four models.

In Figure 7a, the observed values of  $\bar{k}_t$  for the MMA/VAc system are compared with the four models. For a complete discussion, we have reproduced the  $\bar{k}_t$  data for the styrene (ST)/ethyl acrylate (EA) system in Figure 7b. (At this time,  $\bar{k}_t$  data are available for five more systems.<sup>1-3,10,16</sup> However, those data can be described nearly equally well by all or more than two of the models, not permitting unequivocal discrimination of the models.) Among the four models, models 1 and 2 are conceptually similar, and models 3 and 4 belong to the same group. The first model in each group (1 and 3) assumes that the whole chain is important in determining the "diffusion" of the radical, while the second one in each group (2 and 4) stresses the importance of the terminal unit. A correct answer would fall between these two extremes. Viewed from this point, Figure 7 rather conclusively indicates that the former group of models (1 and 2) fail to describe the experiments.

In particular, the failure of model 1 to describe the MMA/VAc system is most evident. On the other hand, the latter group of models, particularly model 3, seem to describe the two systems reasonably well. Excepting those due to Sato et al.,<sup>10</sup> who observed a seemingly peculiar  $\bar{k}_t$  vs  $f_1$  curve, other  $\bar{k}_t$  data<sup>1-3,16</sup> are describable by either model 3 or 4 (or both), at least approximately.<sup>15</sup>

This seems to indicate that the termination is controlled by one or more units at the chain end. As the number of units of this "active" portion of the chain increases, its composition rapidly approaches that of the whole chain. Namely, it is suggested to write

$$\bar{k}_t^{-1} = C_{n,1}k_{t1}^{-1} + C_{n,2}k_{t2}^{-1} \quad (13)$$

where  $C_{n,1}$  ( $=1 - C_{n,2}$ ) is the composition of the active portion of the chain end comprising  $n$  units ( $C_{\infty,1} = F_1$  and  $C_{1,1} = P_1$ ). The number  $n$  may or may not depend on systems. For sufficiently large  $n$ , the underlying concept becomes similar to that of Ito and O'Driscoll,<sup>16</sup> whose model is numerically close to model 3. A similar concept is also shared by Russo and Munari,<sup>22</sup> who stress the importance of the terminal two units, even though their model itself should be grouped into "chemical" models.

Presumably the termination in copolymerization is a more complicated process in which many other factors would take part. To what extent the simplification embodied by eq 13 is permissible and what is the optimum value of  $n$  are important questions to be answered with more experimental data of high quality.

## References and Notes

- (1) Fukuda, T.; Ma, Y.-D.; Inagaki, H. *Macromolecules* **1985**, *18*, 17.

- (2) Ma, Y.-D.; Fukuda, T.; Inagaki, H. *Macromolecules* **1985**, *18*, 26.
- (3) Fukuda, T.; Kubo, K.; Ma, Y.-D.; Inagaki, H. *Polym. J. (Tokyo)* **1987**, *19*, 523.
- (4) Ma, Y.-D.; Kim, P.-S.; Kubo, K.; Fukuda, T. *Polymer*, in press.
- (5) Davis, T. P.; O'Driscoll, K. F.; Piton, M. C.; Winnik, M. A. *J. Polym. Sci., Polym. Lett. Ed.* **1988**, *27*, 181.
- (6) Davis, T. P.; O'Driscoll, K. F.; Piton, M. C.; Winnik, M. A. *Macromolecules* **1990**, *23*, 2113.
- (7) Davis, T. P.; O'Driscoll, K. F.; Piton, M. C.; Winnik, M. A. *Polym. Intern.* **1991**, *24*, 65.
- (8) Piton, M. C.; Winnik, M. A.; Davis, T. P.; O'Driscoll, K. F. *J. Polym. Sci., Polym. Chem. Ed.* **1990**, *28*, 2097.
- (9) Olaj, O. F.; Schnöll-Bitai, I.; Kremminger, P. *Eur. Polym. J.* **1989**, *25*, 535.
- (10) Sato, T.; Takahashi, K.; Tanaka, H.; Ohta, T.; Kato, K. *Macromolecules* **1991**, *24*, 2330.
- (11) Mayo, F. R.; Lewis, A. M. *J. Am. Chem. Soc.* **1944**, *66*, 1954.
- (12) Fukuda, T.; Ma, Y.-D.; Inagaki, H. *Makromol. Chem., Rapid Commun.* **1987**, *8*, 495.
- (13) Fukuda, T.; Kubo, K.; Ma, Y.-D.; Inagaki, H. *Macromolecules* **1991**, *24*, 370.
- (14) O'Driscoll, K. F. *Polym. Prepr. (Am. Chem. Soc., Div. Polym. Chem.)* **1990**, *31* (2), 399.
- (15) Fukuda, T.; Kubo, K.; Ma, Y.-D. *Prog. Polym. Sci.* **1992**, *17*, 875.
- (16) Ito, K.; O'Driscoll, K. F. *J. Polym. Sci., Polym. Chem. Ed.* **1979**, *17*, 3913.
- (17) Kamachi, M.; Liaw, D. J.; Nozakura, S. *Polym. J. (Tokyo)* **1979**, *11*, 921.
- (18) Yamamoto, T.; Yamamoto, T.; Mito, A.; Hirota, M. *Nihon Kagaku Kaishi (Bull. Chem. Soc. Jpn.)* **1979**, No. 3, 408.
- (19) Kamachi, M. *Adv. Polym. Sci.* **1987**, *82*, 209.
- (20) Atherton, J. A.; North, A. M. *Trans. Faraday Soc.* **1962**, *58*, 2049.
- (21) Greenley, R. Z. In *Polymer Handbook*, 3rd ed.; Brandrup, J., Immergut, E. H., Eds.; Wiley: New York, 1989; Chapter II.
- (22) Russo, S.; Munari, S. *J. Macromol. Sci., Chem.* **1968**, *2*, 1321.